The problem of achieving high second-order nonlinearities in glasses: the role of electronic conductivity in poling of high index glasses

C. Corbari [a], L. C. Ajitdoss [b], I. C. S. Carvalho [c], O. Deparis [d], F. P. Mezzapesa [e], P.G. Kazansky [a], K. Sakaguchi [f]

a Optoelectronics Research Centre, University of Southampton, SO17 1BJ, United Kingdom

b Politecnico di Torino, Dipartimento di Scienza dei Materiali ed Ingegneria Chimica, C.so Duca degli Abruzzi 29, 10129 Torino, Italy

c Departamento de Física, Pontifícia Universidade Católica do Rio de Janeiro, Rua Marquês de São Vicente 225, Gávea, 22453-900 Rio de Janeiro, RJ, Brazil

d Centre de Recherche en Physique de la Matière et du Rayonnement (PMR), Facultés Universitaires Notre-Dame de la Paix (FUNDP), B-5000 Namur, Belgium

e National Nanotechnology Laboratory of INFM-CNR,c/o Distretto Tecnologico, Università del Salento, via Arnesano, I-73100 Lecce (Italy)

f Technical Research Laboratory, Nippon Sheet Glass Co. Ltd., Itami, Hyogo 664-8520, Japan

Abstract

Efficient thermal poling of electronically conducting glass is prevented by the inherent difficulty to record a large electrostatic field within such glasses. To overcome this limitation, a waveguide/substrate configuration has been proposed, in which the glass for poling was deposited as a film of appropriate thickness on a substrate chosen for its higher ionic conductivity. Owing to this configuration, the poling voltage drops entirely across the glass film, allowing high electrostatic field to be recorded in spite of the high electronic conductivity of the glass. The proposed method was demonstrated here in the case of bismuth-zinc-borate glasses, which possess high potential for poling because of their high intrinsic $\chi^{(3)}$. A four-fold enhancement of $\chi^{(2)}$ compared to bulk glass, from ~0.5 to ~2 pm/V, is demonstrated. It is also shown that the $\chi^{(2)}$ values obtained are the highest sustainable by the glass limited by the onset of nonlinear conductivity. The waveguide/substrate configuration intrinsically allows obtaining perfect overlap of the poling induced second-order nonlinearity with the guiding region of the waveguide. An equivalent RC-circuit model describing the poled glass reveals that the value of the poling-induced second-order nonlinearity is strongly dependent on the ratio β between ionic and electronic conductivity. The most promising glass systems for poling are found to be the ones displaying the highest product $\chi^{(3)}\beta$. This work is performed on bismuth-zinc-borate heavy metal oxide glasses but the waveguide/substrate configuration proposed here is likely to be equally successful in enhancing the second-order nonlinearity in high $\chi^{(3)}$ electronic conducting glasses such as for example telluride and chalcogenide glasses.

PACS : 42.70.-Nq ; 72.20-i ; 72.80.-r ;77.22.-d

1 Introduction

Glass is an amorphous material having inversion symmetry on a macroscopic scale and therefore possessing vanishing even-order nonlinear optical susceptibilities. Since second-order nonlinear processes are naturally forbidden in centro-symmetric materials, glass-based integrated optical devices such as electro-optic modulators or frequency converters that would be extremely attractive for their compatibility with silicon technology seem unfeasible. However, the technique of thermal poling is known to produce a permanent second-order nonlinearity ($\chi^{(2)}$) in a variety of glass systems[1-6].

Thermal poling involves subjecting the glass to elevated temperatures under an applied static electric field of the order of few kilovolts [7]. In silica glass the poling process is explained using a charge carrier model [8, 9]. At temperatures of the order of 300 ^{0}C the number of charge carriers available for conduction increases and under the applied static field such carriers, typically Na^+ impurities bonded to Si-O^- non-bridging oxygen hole centres, drift leaving behind a negatively charged region. Since this region is depleted of charge carriers its resistance is larger than the bulk of the glass and, like in a voltage divider, all of the voltage drops across it. The negatively charged region extends only for few microns beneath the positive electrodes. Therefore an extremely large electric field of the order of 10^8 - 10^9 V/m which is close to the breakdown strength of silica is established. When the glass is cooled to room temperature and subsequently the voltage is switched off, the Na^+ ions are frozen in their new positions and with them the electric field, E_{dc}, is permanently stored in the glass. It can be shown that E_{dc} couples with the $\chi^{(3)}$ of the glass to produce an effective second-order nonlinearity according to $\chi^{(2)} = 3\ \chi^{(3)}\ E_{dc}$ [10]. If the value of the breakdown strength of silica (~10^9 V/m [11]) is taken as the upper limit for E_{dc} and taking $\chi^{(3)} = 2 \times 10^{-22}$ $m^2\ V^{-2}$ [12] the

expected second-order nonlinearity induced in silica is 0.6 pm/V in remarkable agreement with the measured values [7, 13, 14].

In silica optical fibres such value of the nonlinearity is sufficient for practical applications as the relatively low values can be compensated by longer interaction lengths possible in optical fibres due to the ease of fabrication and to their low propagation losses [15, 16]. However, in order to become attractive for integrated optics a second-order optical nonlinearity of at least 5 pm/V would be desirable. The aforementioned relationship $\chi^{(2)} = 3\ \chi^{(3)}\ E_{dc}$ indicates the route followed in this work: thermal poling of high $\chi^{(3)}$ glasses.

In previous works the potential for nonlinear optical applications of the bismuth-zinc-borate glass family possessing $\chi^{(3)}$ as high as 30 times the third-order nonlinearity of silica was studied [17, 18]. It was suggested that the induced second-order nonlinearity was scaling with the third-order nonlinearity [17]. However, the highest $\chi^{(2)}$ was found to be only 0.7 pm/V. The $\chi^{(2)}$ decayed by less than 30% over a period of 3 years. The sub-linear growth of the $\chi^{(2)}$ with the $\chi^{(3)}$ was ascribed to the lower breakdown strength of the bismuth-borate glasses compared to silica.

In the present work we show that the second-order nonlinearity in the bismuth-zinc-borate glass system is limited by the presence of electronic conduction. A model that takes into account both ionic and electronic conduction is proposed and it is shown to successfully explain the low value of $\chi^{(2)}$ found in the poling of bulk bismuth-zinc-borate glasses. Based on the understanding offered by the model, a route to achieve the maximum nonlinearity in the glass system under study is proposed and demonstrated. A novel sample configuration for poling, comprising of a bismuth-zinc-borate thin film sputtered on a glass substrate offering lower electrical resistance than the film is shown to produce a 4-fold enhancement of the

induced $\chi^{(2)}$. Since this sample geometry is the one of a planar waveguide, it is intrinsically highly compatible with integrated optic devices. Moreover, the maximum $\chi^{(2)}$ is obtained over a broad range of parameters and the overlap between the guided mode and the nonlinear region is crucially always ensured. Furthermore, the model proposed indicates the composition in the ternary bismuth-zinc-borate glass-system resulting in the highest $\chi^{(2)}$. Finally, experimental investigation involving both optical and electrical measurements proved that further enhancement of the SON beyond the values achieved in this work is prevented by the onset of a nonlinear conductivity. It is believed that the model as well as the poling configuration proposed in this work is not restricted to the bismuth-zinc-borate glass system. On the contrary the waveguide/substrate configuration providing the highest possible nonlinearity should be successfully applicable to any electronic conducting glass.

2 Theoretical Constraints

In an earlier paper the poling of glass plates in the bismuth-zinc-borate ternary group was shown to create a nonlinear region close to the surface that had been in contact with the anode electrode suggesting that positive ions play a significant role in the conduction process [17]. Bismuth-borate glasses are also known to exhibit polaronic conduction whereby electrons hop between the two valence states of bismuth [19]. Although the $\chi^{(3)}$ of these glasses can be as high as 30 times the one of silica glass (in BZH2), the induced $\chi^{(2)}$ did not scale up with the third-order nonlinearity. Rather the opposite, the SON in optimised poling conditions was maximised to 0.7 pm/V which does not represent a significant increase compared to the $\chi^{(2)}$ that can be obtained in poled silica.

A better understanding of this apparently puzzling result is provided by modelling the glass as an equivalent RC-circuit while taking into account both ionic and electronic conduction process. The poling process produces two distinct regions in the glass: the depletion region, which is depleted of charge carriers, and the bulk of the sample. Both these regions are characterised by their respective electrical resistance and capacitance. However, at the steady state, the voltage drop across the depletion region, V_d, and across the bulk, V_b, are determined by the resistive properties only (Figure 1). For generality it is assumed that the glass presents both ionic and electronic conduction mechanism assumed to be independent from each other. Hence, the ionic and electronic resistance in the depletion region (R_d^i and R_d^e respectively) and in the bulk (R_b^i and R_b^e respectively) are assumed to be in parallel.

The current running through the circuit is given by the Ohm's law: $I = V / R^{eq}$, where $R^{eq} = R_d^{eq} + R_b^{eq}$ symbolises the equivalent resistance of the whole circuit and R_d^{eq} and R_b^{eq} the equivalent resistance of the depletion layer and bulk respectively. During poling, the electro-static field across the ion-depleted region is given by the voltage drop across the depleted layer divided by its thickness t_d: $\hat{E}_{dc} = V_d / t_d$. After poling, that is after removal of the external field, the stored field is $E_{dc} = \hat{E}_{dc} - V / L$ where L is the glass thickness.

It follows that after poling:

$$E_{dc} = \frac{V_d}{t_d} - \frac{V}{L} = \frac{I \times R_d^{eq}}{t_d} - \frac{V}{L} = \frac{V}{t_d} \frac{1}{1 + \frac{R_b^{eq}}{R_d^{eq}}} - \frac{V}{L} \qquad (1)$$

Bearing in mind that the dominant resistance in a parallel circuit is the smallest the model can be tested on two extreme cases:

a) ionic conductor (e.g. silica): In an ionic conductor the electronic conductivity is assumed to be negligible compared to the ionic conductivity: $R_{d,b}^{i} << R_{d,b}^{e} \Rightarrow R_{d,b}^{eq} \approx R_{d,b}^{i}$. It is also assumed that the resistance in the depleted region is much larger than in the bulk owing to the smaller number of charge carriers: $R_d^i >> R_b^i \Rightarrow R_d^{eq} >> R_b^{eq}$. Therefore from eq.(1) $E_{dc} \approx V / t_d$ for $L >> t_d$. It follows the well known result that in an ionic conductor all the applied voltage drops across the thin depletion region.

b) electronic conducting glass: The conduction is dominated here by the electronic conductivity $R_{d,b}^{e} << R_{d,b}^{i} \Rightarrow R_{d,b}^{eq} \approx R_{d,b}^{e}$. It is also assumed that the electronic conductivity

is the same in both bulk and depletion region. As a consequence of the last hypothesis the bulk and electronic resistance scale with their respective length $R_b^{eq} \approx R_b^e = R_d^e \times (L - t_d)/t_d$. It is further assumed that e^- injection at the cathode prevents the formation of a charge depleted region adjacent to the surface in contact with the cathode electrode. It follows from eq.(1):

$$E_{dc} \approx \frac{V}{t_d} \frac{1}{1 + \frac{R_d^e \left(\frac{L - t_d}{t_d} \right)}{R_d^e}} - \frac{V}{L} = 0 \qquad (2)$$

After poling no electro-static field can be stored in an electronic conducting glass unless, other phenomena like structural modifications, charge injection at the anode or bond orientation are also occurring. Compared to an ionic conducting glass the advantage of using a high $\chi^{(3)}$ - glass is considerably reduced.

c) mixed ionic/electronic conducting glass: the behaviour of the glass in this intermediate situation is described by the ratio between electronic and ionic (bulk) conductivity: $\beta = \sigma_b^i / \sigma^e$. As in the case of an ionic conductor the condition $R_d^i >> R_b^i$ applies. Moreover, by recalling the microscopic interpretation of the electrical resistance $R = \sigma^{-1} L / S$ with L being the length of the resistor (thickness of the glass in the case under consideration) and S being the sample cross-section (electrode area) it can be shown that $R_b^{eq} = R_b^i \times \beta / (1 + \beta)$. Furthermore, with $R_d^{eq} \approx R_d^e$, it follows:

$$E_{dc} \approx \frac{V}{t_d} \frac{1}{1+\frac{1}{1+\beta}\left(\frac{L-t_d}{t_d}\right)} - \frac{\mathrm{V}}{\mathrm{L}} \qquad (3)$$

This equation reduces to the limit of an ionic conducting glass for $\beta \to \infty$ and to the limit of an electronic conducting glass for $\beta \to 0$.

The above considerations suggest that a dependence of the frozen-in field on the sample thickness (L) should be observed while poling an electronic as well as mixed ionic/electronic conducting glass (eqs. 2 and 3). Such dependence has been experimentally confirmed in [17, 20]. The data from table 2 of [17] on the poling of bulk glasses, reported here in Table 1 for convenience, can be reinterpreted in light of the RC-model proposed in these pages.

The first observation is that the values of $\chi^{(2)}$ obtained in BZH4 and BZH7 is ~ 10 times as large as the nonlinearity predicted using eq.(2) that describes the poling of a purely electronic conducting glass. In line with the observation made at the beginning of this section that positive ions plays an important role in the poling process of bismuth-zinc-borate glasses we conclude that this glass system exhibits a mixed ionic and electronic conductivity. The frozen-in field in bulk BZH* glasses is calculated in Table 1 according to the rectification model, $\chi^{(2)} = 3\ \chi^{(3)}\ E_{dc}$, based on the values of the maximum induced SON. For the BZH2, BZH7 and BZH4 glass the frozen-in field is estimated in 4 x 10^7, 5 x 10^7 and 6 x 10^7 V/m respectively. The factor β, introduced earlier to express the ratio between the ionic and electronic bulk conductivity, and determined according to eq. (3) is found as 2, 12.5, 15.5 and 16.8 for the BZH2, BZH7, BZH4 and BZH6 glass respectively (Table 1). Not surprisingly the

glass with larger bismuth content displays β close to zero which is the limit for an electronic conducting glass.

In the limit $L >> t_d$, eq.(3) shows that the maximum frozen-in field in bulk bismuth-zinc-borate glasses is a multiple β of the applied field: $E_{dc}\big|_{MAX} \approx E_{applied} \times \beta$. The multiplication factor being higher the lower is the electronic conductivity of the glass. As a consequence of the above expression: $\chi^{(2)}_{MAX} \approx 3E_{applied}\left[\chi^{(3)} \times \beta\right]$. Owing to electronic conduction, the maximum SON in bulk bismuth-zinc-borate glasses is limited by the externally applied poling field and hence, for a fixed poling voltage, by the sample thickness. Interestingly the product $\chi^{(3)} \times \beta$ which depends solely upon material properties gives a useful figure-of-merit to predict the performance of bismuth-zinc-borate glasses for poling. The product is larger for BZH7 compared to the other composition studied indicating that higher nonlinearities are to be expected in this glass composition (Table 2). Note that, according to the model presented here, the higher $\chi^{(2)}$ of BZH2 in Table 1 is due to the 5 times lower thickness compared to the other samples under study rather than to its higher $\chi^{(3)}$. Taking a step further it is possible to infer from the available data the glass composition in the bismuth-zinc-borate ternary glass system that would have provided the highest $\chi^{(2)}$. The bismuth concentration that maximise the product $\chi^{(3)} \times \beta$ is found by extrapolating the variation of $\chi^{(3)}$ and β with the bismuth content from the data in Table 1 by polynomial fitting. The best composition is found for $[Bi_2O_3]$ = 14.6mol% which is not far off BZH7 glass. In the following our experimental results will prove that indeed BZH7 shows higher SON than BZH4 and BZH2 glasses.

Once the role of the electronic conductivity has been identified as the factor responsible for the low nonlinearity induced in bulk glasses, it is possible to propose in the present work a route allowing effective poling of electronic conducting glasses. The relationship

$\chi^{(2)}_{MAX} \approx 3E_{applied}\left[\chi^{(3)} \times \beta\right]$ found above suggests that once $\chi^{(3)}$ and β have been fixed by the choice of the material the only parameter available to enhance the second-order nonlinearity is the externally applied field which can be maximised by choosing $L \to t_d$ that is by reducing L to the order of few microns.

Such thin samples require the use of opportunely chosen substrates. The ideal one has to ensure that all of the externally applied voltage drops across the high $\chi^{(3)}$-glass film to be poled. Moreover by choosing a substrate possessing lower refractive index than the film a planar waveguide configuration is simultaneously realised.

The solution proposed here involves the sputtering of μm-thick high $\chi^{(3)}$ glass films on top of suitable substrates. From the electrical point of view, the thin-film deposited onto a dielectric substrate can be treated with the Maxwell-Wagner model describing the repartition of the applied voltage between two dielectric layers in a capacitor [21]. At steady state ($t \to \infty$), the capacitances behave like open circuits and the externally applied voltage, V is distributed following $V_1 = VR_1 / \left(R_1 + R_2\right)$ where V_1 is the voltage drop on the film and R_1 and R_2 represent the equivalent resistances of film and substrate respectively [21]. The way to maximise V_1 is therefore to use a high ionic conductive glass substrate such that $R_1 >> R_2$. With the externally applied voltage dropping mainly across the high $\chi^{(3)}$ glass film, the frozen-in electric-field, and hence $\chi^{(2)}$, is localised within the film. The overlap of the nonlinear region with the guided optical mode is therefore ensured in this configuration. The frozen-in field is given by eq.(2) with L equal to the film thickness t_{film} should the film possesses only electronic conductivity. In the case of mixed ionic-electronic conductivity, the

frozen-in field is given by eq.(3) with L equal to t_{film} and t_d equal to the ion-depleted layer in the film.

It should be noted however that the maximum field that the glass can withstand is limited by the breakdown strength of the glass itself. For example, in an ionic conductor such as a silica film deposited on a high ionic conductive substrate, even though the applied voltages could produce electric fields in excess of 10^9 V/m across the film the maximum $\chi^{(2)}$ would is still limited to ~0.6 pm/V by the breakdown strength of the silica glass.

3 Experimental procedures

3.1 Glass samples

The glass compositions used in this work have been developed by Nippon Sheet Glass Ltd. The glass samples (BZH*) were fabricated by melting and quenching in the ternary Bi_2O_3-ZnO-B_2O_3 system. Boron and Zinc acted as network former and modifier respectively. The bismuth oxide content was varied from 6.25mol% to 25mol% while keeping the ratio r = $[ZnO]_{mol\%}/([ZnO]_{mol\%}+[B_2O_3]_{mol\%})$ constant and equal to 0.5. The BZH4, BZH7 and BZH2 glasses contain 6.25mol%, 12.5mol% and 25mol% of bismuth respectively and possess refractive index of 1.7, 1.8 and 1.9 respectively.

The third-order nonlinearity of BZH2 had been measured at 1064nm by Gomes et al. and found to be 60 x 10^{-22} m^2/V^2 that is 30 times higher than the $\chi^{(3)}$ in silica glass [22]. The $\chi^{(3)}$ of BZH7 and BZH4 is estimated from the refractive index using the Miller's rule [10] and found to be 33 x 10^{-22} m^2/V^2 and 16.5 x 10^{-22} m^2/V^2 respectively.

The BZH* glasses were deposited on 150 μm thick sodium-borosilicate substrate (Schott D263 M) by radio-frequency sputtering. The RF power was 250W, the chamber temperature was kept to 20°C in a Ar/O_2 atmosphere at the pressure of 20 mTorr. Nominal film thicknesses of 2,3, 4 and 5 μm have been realised for the experiments. Borosilicate glass was chosen as substrate as a widely available glass satisfying the criteria of high conductivity and having refractive index of 1.52, lower than the BZH* films. Prism coupling measurements performed with the 3 μm BZH7 film showed that the structure formed a planar waveguide although multi-moded at 632 nm. Substrates with refractive index closer to the BZH* film

would be better to provide single-mode guidance however in this first work our aim is to prove the validity of the model described in section 2 and to efficiently pole electronic conducting glasses in a structure which can be readily applied to integrated optical devices.

3.2 Poling set-up and procedures

For thermal poling the samples were sandwiched between pressed-in electrodes. Since poling of bismuth-zinc-borate glass is very sensitive to the electrodes' roughness [17], evaporated gold on silicon or polished stainless steel electrodes were employed. Silicon electrodes were avoided because of the occurrence of anodic bonding.

The samples, mounted in a specially designed rig, were placed into an oven chamber where the temperature could be controlled up to ± 1°C. Typical poling temperatures were ranging between 150°C up to 350°C. The poling voltage, in the range of few kilovolts, was applied to the sample through a Glassman High Voltage supply. In the experiments the BZH* films were always kept in contact with the anode. The cathode electrode, which was in contact with the borosilicate substrate, was grounded. An ammeter (Keithley DMM 2000) was inserted in series between the cathode and the ground, protected by a 100kΩ resistance.

3.3 Non-linearity evaluation method

The value of the $\chi^{(2)}$ induced by poling in the glass was measured using the classical Maker's fringe technique (MFT) [23]. A Nd:YVO_4 solid state laser (Lumera SuperRapid) operating at 1064 nm and delivering 8 ps at the repetition rate of 500 kHz was used as pump. The samples were mounted on a computer controlled 3-axis plus rotation stage. The laser light was focused onto the sample under investigation and the second-harmonic that was produced was

carefully separated from the pump by means of dichroic mirrors and narrow band filters and finally measured with a silicon detector (Newport 918SL).

In order to avoid surface damage to the samples or else erase the nonlinearity because of the high peak-powers the average power was kept below 250 mW. The second-order nonlinearity was estimated relative to α-quartz crystal (d_{11} = 0.3 pm/V [24]). The thickness of the nonlinearity was measured independently using the stack Maker's fringe technique (SMFT) proposed in [25]. For this measurement the poled sample is split in two halves which are then pressed in contact with the anode surfaces facing each other. The Maker's fringe pattern is then recorded for the sandwich structure (SMFT) as well as for the single poled glass (MFT). The length of the nonlinear layer (t_d) is determined from:

$$t_d = \frac{2}{\pi} l_c \cos(\vartheta_{2\omega}) \arcsin\left(\frac{1}{2}\sqrt{\frac{P_{SMFT}^{2\omega}}{P_{MFT}^{2\omega}}}\right) \tag{4}$$

where the coherence length l_c is taken to be 7.39 μm for BZH7, 13.3 μm for BZH4 and 6.2 μm for BZH2, $\theta_{2\omega}$ is the internal angle of incidence and $P^{2\omega}$ is the SHG power for MFT (single glass) and SMFT (sandwich of two glasses).

3.4 Electrical measurements

Accurate current measurements were taken with a guard electrode configuration. The samples were first cleaned for 5 minutes in acetone at 50°C in an ultrasonic bath followed by further 5 minutes in isopropanol. Then they were dried with methanol and blow dried with nitrogen flow. Finally they were placed in an oven at 120°C for 30 minutes to remove traces of moisture before evaporating gold electrodes on their surfaces. The anode electrode had a diameter of 13 mm whereas the inner cathode electrode had a diameter of 7 mm. The guard ring around the cathode was 13 mm outer and 8 mm inner diameter.

4 Results

Confirmation that the film-on-substrate configuration allows the nonlinearity to be entirely localised within the film, was obtained by poling a 3.0 μm BZH7 film on 1 mm borosilicate substrate in the conditions quoted for Exp #1 in Table 2. After poling, the sample was immersed in diluted nitric acid which etches the bismuth-zinc-borate glass but leaves the borosilicate unaffected. As a consequence of its weakened adhesion to the substrate, the film could be mechanically removed from half of the borosilicate plate. After, the sample was mounted on the MFT set-up described in section 3.3 and tested for SHG. To this purpose the laser light was scanned across the poled region whilst keeping the sample at the fixed angle of 60^{o} (Figure 2). Starting from outside the poled region, the measured SHG signal increased as soon as the laser spot reached the boundary of the poled region. The fluctuations in the SHG intensity in the poled regions were caused by the etching process. The position of 7.8 mm marks the boundary between the region with the film (< 7.8 mm) and the region where the film had been removed (> 7.8 mm). The abrupt drop in the SHG power observed as the laser light crossed the boundary indicates that the SH light is not produced within the substrate. It is therefore concluded that the nonlinearity is confined within the film.

A second set of experiments was designed to test the dependence of the SON from the thickness of the film as predicted by eq.(2) and eq. (3). BZH7 films of 1.0, 1.5, 2.0 and 3.0 μm were sputtered on 150 μm borosilicate substrate, thermally poled and characterised for second-harmonic generation using the MFT (Exp #2 in Table 2). The thickness of the nonlinear region was measured independently by the SMFT and found to equal the film thickness in accordance with Exp #1 and with the model that was proposed earlier (Figure 3 and Figure 4). Once the thickness of the nonlinear region was determined the $\chi^{(2)}$ could be

evaluated from the MFT curves. Unexpectedly, within 3 times the standard deviation, σ, of the experimental errors, the second-order nonlinearity was the same in all samples, and estimated in 1.73 ± 0.04 pm/V by weighted average (Table 2). Longer poling times, 1000 sec. against 30 sec. resulted again in the same induced SON (Table 2).

Analogues measurements in BZH4 and BZH2 glasses confirmed the same trend (Exp #3 in Table 2). Borosilicate substrates 150 μm were sputtered with 2 and 3 μm of BZH2 and BZH4. Poling was performed at 150^{o}C for 60 sec. with 2.5 kV applied. As before the thickness of the nonlinearity were measured via the SMFT technique. In both glass compositions the $\chi^{(2)}$ was found to be localised in the film and independent of the film thickness. The weighted average of the MFT measurements indicated $\chi^{(2)}$ ~1.20 ± 0.05 pm/V and ~1.14 ± 0.02 pm/V in BZH4 and BZH2 respectively (Figure 5 and in Table2). For comparison poling of 3 μm –thick BZH7 film on borosilicate at 150^{o}C produced 1.50 ± 0.06 pm/V (Exp #3 in Table 2).

Poling at higher voltages did not result in an appreciable increase of the induced second-order nonlinearity (Exp #4 in Table 2). Borosilicate substrates with 3 μm BZH4 and BZH2 films were poled in the same conditions as above except for the voltage which was now set to 4.0 kV. The $\chi^{(2)}$ was measured to be 1.24 ± 0.07 pm/V in BZH4 and 1.03 ± 0.03 pm/V in BZH2 (Figure 5) which are, within the experimental uncertainty, comparable to the measured values for the samples poled at 2.5 kV. BZH7 glass composition presented the same behaviour: poling of BZH7 film under the same conditions as for Exp #2 aside for the larger poling voltage of 4.0 kV resulted in the establishment of SON of 1.88 ± 0.26 pm/V as for poling at 2.5 kV. The dependence of the second-order nonlinearity from the poling voltage was further investigated by poling a series of identical BZH7 3-μm film on 150 μm borosilicate

substrates at 150°C for 60 seconds and in a range of different voltages (Exp #5 in Table 2). The induced $\chi^{(2)}$ was found to saturate at high voltages (Figure 6).

The results presented so far point out that the nonlinearity induced in the BZH* film on borosilicate substrate reached its maximum value. Understanding the limiting factor is key to further improve the nonlinearity in poled glasses. Moreover it is a general problem not necessarily confined to the bismuth-zinc-borate glass system investigated in this study. Silica glass is the most characterised material for poling and as discussed in the introduction, the $\chi^{(2)}$ is believed to be limited by the breakdown strength of the glass to 0.6 pm/V. The structure we have proposed having a μm-thick film of silica sputtered on a substrate having lower electrical resistance allows producing electric fields in excess of the breakdown strength of silica ~10^9 V/m across the film. Poling of 1 μm film of silica deposited on 150 μm borosilicate substrate at 4.0kV for 600 seconds at the temperature of 240 °C resulted in the production of a second-order nonlinearity of 0.7 pm/V confined within the silica film. The value is compatible with a SON limited by the breakdown strength of silica.

Insight into the factor limiting the nonlinearity in BZH* glasses is gained through current measurements. Current measurements were taken while poling the sample for Exp #5 at 500V, 750V, 1000V and 1500V (Figure 7). All curves present an initial spike-like feature which is due to the displacement current caused by the polarisation of the dielectric. The decay of the current observed after 60 seconds from the beginning of poling marks the beginning of the cooling phase, and it is caused by the increase in resistance as the temperature decreases. A more interesting feature is the difference in the current dynamics between low (< 1kV) and high voltages (> 1kV). For poling voltages below 1kV the current is seen to decrease with time. This trend which is seen also in ionic conducting glasses is

generally interpreted as the formation of a region inside the glass which is depleted of charge carriers and it is therefore more resistive than the rest of the glass [26]. In silica this region is created by the migration of Na^+ impurities. The current trace that refers to the poling at 1500V, though, shows a completely different behaviour: it increases with time. Because of the low levels of current (<1 μA) the heating caused by Joule effect is negligible. The current measurements shown in Figure 7 seem to indicate that a different conduction mechanism is taking place at higher voltages [26]. We note as well that above 1500V the induced second-order nonlinearity appears to saturate to its maximum value (Figure 6).

This feature was further investigated in a second set of experiments where the I-V curves were measured for BZH4 sputtered on borosilicate with 2, 3, and 4 μm thickness respectively. BZH4 films on borosilicate samples were prepared with evaporated electrodes in a guard electrode configuration. The borosilicate glass used as a substrate was also prepared in the same fashion. For each sample 2 or 3 data sets were taken (Figure 8). In all the samples that have been tested the current first increases linearly with the externally applied voltage. In agreement with the observation made earlier above a certain voltage threshold the current deviates from a linear behaviour. In Figure 8 data have been fitted to a straight line for voltages below the threshold voltage. The linear behaviour is then extrapolated to higher voltages in order to highlight the deviation from the linear behaviour (dashed line). The current measured above the voltage threshold exhibits a quadratic increase with the applied voltage. In each graph, data points above the threshold are fitted to a parabola. As a boundary condition, the parabola is imposed to be tangent to the linear increase of the current for low voltages. The threshold voltage can therefore be defined as the tangent point of the parabola with the straight line. In the 2, 3, 4 μm BZH4 film on 150 μm borosilicate samples the

threshold voltage defined as above is found to be 500 ± 3 V, 1005 ± 4 V, and 1110 ± 7 V respectively.

5 Discussion

All the poling experiments carried out on BZH2, BZH4 and BZH7 glass compositions using the waveguide/substrate configuration clearly indicate that the nonlinearity and hence the static electric field is localised within the film. Exp#1 showed that the thickness of the substrate is irrelevant provided that the substrate electrical resistance is higher than the one offered by the film. Moreover, the film-on-substrate configuration was proved in Exp#2 and Exp#3 to be successful in enhancing the second-order nonlinearity compared to bulk glasses. Second-order nonlinearity of 1.95 ±0.13 pm/V was obtained in BZH7 using the novel configuration against 0.5 pm/V in bulk BZH7 [17].

All experiments indicate that the frozen-in field drops across the whole thickness of the film and also that the value of the nonlinearity is the same irrespective of the thickness of the film. Because of the direct correspondence between $\chi^{(2)}$ and the frozen-in field, ($\chi^{(2)} = 3\,\chi^{(3)}E_{dc}$), we can make the assumption that the frozen-in field is limited to a maximum value. Such an assumption is justified also in light of the fact that poling at low voltages induces second-order nonlinearity which increases with the applied voltage (It would be a linear dependence according to eq.(3)) before saturating when the external voltage is above 1500V-2000V (Figure 6). In the saturation regime the second-order nonlinearity in BZH7 is ~1.5 pm/V corresponding to a stored field of 1.5 x 10^8 V/m, 5 -10 times lower than the fields of ~10^9 V/m obtained by poling silica glass.

In poled silica it is well known that the second-order nonlinearity is limited by the breakdown strength of the glass (~10^9 V/m). It was shown in this work that in a silica film sputtered on borosilicate this limit value is easily reached (Exp#6). However, capacitance-voltage measurement of the breakdown strength in BZH7 made for this work, although not presented here, showed that breakdown starts at 6 x 10^8 V/m. It should therefore be possible to achieve nonlinearities up to 6 pm/V in BZH7. The fact that these values were not reached in this work was because another mechanism comes into play before breakdown is reached.

Evidence was provided in Figure 7 and Figure 8 that the current dynamics abruptly change above a certain voltage threshold. In light of the assumption that the frozen-in field is limited to a maximum value, the moment of transition may be interpreted as triggered by an electric field intensity threshold rather then a voltage threshold. The experimentally verifiable consequence of this statement is that the electric field threshold is expected to be the same for all samples irrespective of the film thickness. The voltage threshold identified in Figure 8 refers to the externally applied voltage. In accordance with the Maxwell-Wagner double layer condenser model, the corresponding voltage drop across the film can be calculated from $V_1 = VR_1 / \left(R_1 + R_2 \right)$. The substrate electrical resistance R_2 is measured as 0.25 GΩ from the current measurements on the borosilicate plate. The film resistance R_1 is determined from the data shown in Figure 8 in the Ohmic regime at low voltages. For the 2, 3 and 4 μm thick films, R_1 is measured as 1.62 ± 0.08 GΩ, 1.84 ± 0.16 GΩ , 5.32 ± 0.49 GΩ, respectively. The film resistance is almost 10 times larger than the substrate resistance and confirms the good choice of the borosilicate as a substrate. The films of nominal thickness 2, 3 and 4 μm were accurately measured with a profilometer and found to be 1.82, 2.72 and 3.55 μm. The fact that R_1 does not seems to scale with the thickness of the film in

our measurement is likely to be caused by batch to batch variations which introduced systematic errors not considered in our error analysis. However, error propagation indicates that the error in V_1 is minimally affected by the error in R_1. The voltage drop across the film corresponding to the change in the current dynamics occurring for the externally applied voltage of 500 V, 1005 V and 1110 V (Figure 8) is determined as 430 ± 4 V, 885 ± 10 V and 1060 ± 8 V respectively. Approximately 90% of the externally applied voltage drops across the film before current runaway. The electric field intensity in the film $E_{dc} = V_1 / t_{film}$ where t_{film} is the film thickness is calculated as (2.37 ± 0.02) x 10^8 V/m for the 1.82 μm film, (3.25 ± 0.04) x 10^8 V/m for the 2.72 μm film, and (2.99 ± 0.02) x 10^8 V/m for the 3.55 μm film. The data are compatible with the existence of an electric field threshold beyond which current runaway occurs thus limiting the maximum electric field that can be frozen in the glass. The electric field threshold can be estimated in (2.87 ± 0.26) x 10^8 V/m corresponding to a SON of 1.41 ± 0.12 pm/V which is in remarkably good agreement with the value measured with the Maker's fringe technique of 1.20 ± 0.04 pm/V.

The agreement between nonlinear optical measurements and the current measurements allows us concluding that the onset of the nonlinear conductivity is limiting the second-order nonlinearity in BZH4 glass.

6 Conclusion

Glass compositions presenting electronic conductivity typically possess third-order nonlinearity order of magnitudes higher than silica glass. Nonetheless poling of these glass compositions has so far resulted in recording second-order nonlinearity much smaller than what expected from the rectification model $\chi^{(2)} = 3\ \chi^{(3)}\ E_{dc}$ [1, 2, 17]. In this work, by

analysing results in the bismuth-zinc-borate ternary glass, which is characterised by both ionic and polaronic conduction, we have identified the cause of the low nonlinearity in the electronic conductivity which prevents high fields to be recorded in the glass. An equivalent RC-circuit model describing the poled glass with mixed ionic and electronic conductivity was introduced and a route to achieve the highest $\chi^{(2)}$ sustainable by the glass was proposed and experimentally demonstrated. The poling induced $\chi^{(2)}$ in electronic conducting glass is shown to depend upon the product of $\chi^{(3)}$ and the ratio β between ionic and electronic conductivity. Therefore for the purpose of obtaining glasses with the highest second order nonlinearity the high $\chi^{(3)}$ is only one part of the equation. Controlling or limiting the electronic conductivity is an equally important factor. This point is highlighted in this work by poling bismuth-zinc-borate glasses of varying composition resulting in changing both $\chi^{(3)}$ and the ratio between ionic and electronic conductivity. The highest nonlinearity is obtained in the glass composition maximising the product $\chi^{(3)}\beta$. The $\chi^{(2)}$ is also found to be dependent on the intensity of the externally applied poling field. The film-substrate configuration was intentionally introduced as a method to force the electric-field to be frozen on a micron-size thickness with a consequent enhancement of the induced nonlinearity compared to a thick bulk glass. The substrate has to be chosen with lower resistance than the film and if also chosen with lower refractive index the proposed configuration, being the one of a planar waveguide, is very much suitable for integrated optical devices based on poled glasses. The film/substrate configuration presents several advantages: first of all it ensures that the maximum $\chi^{(2)}$ sustainable by the glass is reached and that it is reached in a broad range of parameters making it easy to compare different glass compositions and film thicknesses. Secondly, it ensures a perfect overlap between the nonlinearity and the guided mode of the waveguide.

In summary the poling of semiconducting bismuth-zinc-borate glasses in the planar waveguide configuration proposed in this work with properly selected substrate enabled a four-fold enhancement of $\chi^{(2)}$ compared to bulk with the nonlinearity perfectly overlapped with the guiding region of the waveguide. Such configuration may prove advantageous to further enhance the second-order nonlinearity in poled high $\chi^{(3)}$ semiconducting glasses such as telluride and chalcogenide glasses where 2 pm/V and 8 pm/V respectively have been obtained in bulk glasses [1, 2]. The RC-circuit equivalent model introduced here that was successful in predicting the best composition among the bismuth-zinc-borate ternary system may provide invaluable guidance in the choice of the glass composition.

References

[1] K. Tanaka, A. Narazaki and K. Hirao, *Optics Letters* 25 (2000), p. 251.

[2] M. Guignard, V. Nazabal, F. Smektala, J. L. Adam, O. Bohnke, C. Duverger, A. Moreac, H. Zeghlache, A. Kudlinski, G. Martinelli and Y. Quiquempois, *Adv. Funct. Mater.* 17 (2007), p. 3284.

[3] V. Nazabal, E. Fargin, C. Labrugere and G. Le Flem, *Journal of Non-Crystalline Solids* 270 (2000), p. 223.

[4] H. Nasu, H. Takeda, T. Hashimoto and K. Kamiya, *Journal of the Ceramic Society of Japan* 113 (2005), p. 555.

[5] Y. Quiquempois, A. Villeneuve, D. Dam, K. Turcotte, J. Maier, G. Stegeman and S. Lacroix, *Electronics Letters* 36 (2000), p. 733.

[6] Y. Menke, M. Ferraris, C. Corbari and J. Fage-Pedersen, *Journal of Non-Crystalline Solids* 345-46 (2004), p. 366.

[7] R. A. Myers, N. Mukherjee and S. R. J. Brueck, *Optics Letters* 16 (1991), p. 1732.

[8] A. Kudlinski, G. Martinelli and Y. Quiquempois, *Optics Letters* 30 (2005), p. 1039.

[9] A. Kudlinski, Y. Quiquempois and G. Martinelli, *Optics Express* 13 (2005), p. 8015.

[10] R. W. Boyd, Nonlinear Optics, Elsevier.

[11] S. M. Sze, Physics of Semiconductors Devices, Wiley, (1981).

[12] R. Adair, L. L. Chase and S. A. Payne, *Journal of the Optical Society of America B-Optical Physics* 4 (1987), p. 875.

[13] D. Faccio, V. Pruneri and P. G. Kazansky, *Applied Physics Letters* 79 (2001), p. 2687.

[14] Y. Quiquempois, N. Godbout and S. Lacroix, *Physical Review A* 65 (2002).

[15] G. P. Agrawal, Nonlinear Fiber Optics, Academic Press.

[16] C. Corbari, A. Canagasabey, M. Ibsen, F. Mezzapesa, C. Codemard, J. Nilsson and P. G. Kazansky, All-fibre frequency conversion in long periodically poled silica fibres, *2005 Optical Fiber Communications Conference Technical Digest*, Ieee, Anaheim, CA, (2005).

[17] O. Deparis, F. P. Mezzapesa, C. Corbari, P. G. Kazansky and K. Sakaguchi, *Journal of Non-Crystalline Solids* 351 (2005), p. 2166.

[18] W. Yang, C. Corbari, P. G. Kazansky, K. Sakaguchi and I. C. S. Carvalho, *Optics Express* 16 (2008), p. 16215.

[19] S. P. Yawale and S. V. Pakade, *Journal of Materials Science* 28 (1993), p. 5451.

[20] F. P. Mezzapesa, I. C. S. Carvalho, C. Corbari, P. G. Kazansky, J. S. Wilkinson, G. Chen and Ieee, Voltage-assisted cooling: a new route to enhance Chi((2)) during thermal poling, *Conference on Lasers and Electro-Optics (CLEO)*, Optical Soc America, Baltimore, MD (2005).

[21] J. C. Anderson, Dielectrics, Chapman and Hall, London (1964).

[22] A. S. L. Gomes, E. L. Falcao, C. B. de Araujo, D. Rativa, R. E. de Araujo, K. Sakaguchi, F. P. Mezzapesa, I. C. S. Carvalho and P. G. Kazansky, *Journal of Applied Physics* 101 (2007).

[23] J. Jerphagnon and S. K. Kurtz, *Journal of Applied Physics* 41 (1970), p. 1667.

[24] V. G. Dmitriev, G. G. Gurzadyan and D. N. Nikogosyan, Handbook of Nonlinear Optical Crystals, Springer, (1997).

[25] C. Corbari, O. Deparis, B. G. Klappauf and P. G. Kazansky, *Electronics Letters* 39 (2003), p. 197.

[26] M. Fokine, F. D. Moreira and I. C. S. Carvalho, Poled glasses for optical devices - art. no. 709918, In: Photonics North 2008, Réal Vallée, Michel Piché, Peter Mascher, Pavel Cheben, Daniel Côté, Sophie LaRochelle, Henry P. Schriemer, Jacques Albert, Tsuneyuki Ozaki, Eds., Proc. of SPIE Vol. 7099, 709918, (2008)

Captions

Table 1

Data of $\chi^{(2)}$ are after table 2 in ref. [17] for the poling of BZH2, BZH7, BZH4 and BZH6 bulk glasses. L: sample thickness, t_d: thickness of the depletion region, V: poling voltage, $\chi^{(3)}$ of BZH2 was measured in [22]. $\chi^{(3)}$ of BZH7, BZH4 and BZH6 estimated according to Miller's rule (see section 3.1). E_{dc}: frozen-in field induced by poling calculated according to $\chi^{(2)} = 3\ \chi^{(3)} E_{dc}$. β: ratio between ionic and electronic bulk conductivity calculated according to eq.3.

Table 2

Summary of the poling results of BZH* films on borosilicate substrate.

Figure 1

Scheme of the structure of the glass after poling. The equivalent d.c. electrical circuit is represented in the scheme on the right.

Figure 2

SHG scan across the poled region in 1.5 μm BZH7 film on 1.0 mm borosilicate substrate. The BZH7 film had been removed in the region on the right of the black vertical line (>7.8 mm). In such region no SHG is produced indicating that the nonlinearity is localised in the nonlinear layer.

Figure 3

Poling of 2 μm BZH7 film deposited on 150 μm borosilicate substrate at 150 ºC for 60 sec. with 2.5 kV applied. (top) MFT and SMFT curves.. (bottom) The thickness of the nonlinear region is found as 2 μm, equal to the thickness of the BZH7 film.

Figure 4

Poling of 3 μm BZH7 film deposited on 150 μm borosilicate substrate at 150 ºC for 60 sec. with 2.5 kV applied. (top) MFT and SMFT curves. (bottom) The thickness of the nonlinear region is found as 3 μm, equal to the thickness of the BZH7 film.

Figure 5

MFT measurements of BZH2 and BZH4 films on 150 μm substrate. Poling temperature 150 ^{o}C, poling time 60 sec. Poling voltage is indicated in the graphs' legends. (◊) Experimental data. (solid line) Fit to the data

Figure 6

BZH7 3 μm film on 150 μm borosilicate substrate. Dependence of $\chi^{(2)}$ from the poling voltage. Poling temperature 150 ^{o}C, poling time 60 sec. Dotted line is a guide for the eye.

Figure 7

BZH7 3 μm film on 150 μm borosilicate substrate. Voltage dependence of the poling current. Poling temperature 150 ^{o}C, poling time 60 sec.

Figure 8

I-V curves in BZH4 film on 150 μm borosilicate substrate showing the onset of nonlinear conductivity.

Sample	Bi_2O_3 (mol%)	L (mm)	$\chi^{(3)}$ (m^2/V^2)	t_d (μm)	V (kV)	$\chi^{(2)}$ (pm/V)	E_{dc} (V/m)	β
BZH2	25.0	0.2	60×10^{-22}	6.2	4.0	0.68	3.9×10^{7}	2.0
BZH7	12.5	1.0	33×10^{-22}	6.0	4.0	0.47	5.0×10^{7}	12.5
BZH4	6.25	1.0	16×10^{-22}	13.3	4.0	0.29	6.7×10^{7}	15.5
BZH6	-	0.9	7.65×10^{-22}	11.0	4.0	0.17	7.4×10^{7}	16.8

Table 1

	Glass	Film thickness (μm)	Substrate thickness (μm)	Voltage (kV)	Temperature (^{o}C)	Time (sec)	$\chi^{(2)}$ (pm/V)
Exp #1	BZH7	3.0	1000	2.5	240	30	1.34 ± 0.05
Exp #2	BZH7	3.0	150	2.5	240	1000	1.78 ±0.07
Exp #2	BZH7	1.5	150	2.5	240	1000	1.82 ±0.25
Exp #2	BZH7	1.0	150	2.5	240	30	1.85 ±0.74
Exp #2	BZH7	1.5	150	2.5	240	30	1.88 ±0.26
Exp #2	BZH7	2.0	150	2.5	240	30	1.95 ±0.13
Exp #2	BZH7	3.0	150	2.5	240	30	1.73 ±0.07
Exp #3	BZH7	3.0	150	2.5	150	60	1.6 ±0.06
Exp #3	BZH4	2.0	150	2.5	150	60	1.25 ±0.18
Exp #3	BZH4	3.0	150	2.5	150	60	1.17 ±0.06
Exp #3	BZH2	2.0	150	2.5	150	60	1.16 ±0.04
Exp #3	BZH2	3.0	150	2.5	150	60	1.13 ±0.03
Exp #4	BZH4	3.0	150	4.0	150	60	1.24 ±0.07
Exp #4	BZH2	3.0	150	4.0	150	60	1.03 ±0.03
Exp #4	BZH7	1.5	150	4.0	240	30	1.88 ±0.26
Exp #5	BZH7	3.0	150	0.5	150	60	-
Exp #5	BZH7	3.0	150	0.75	150	60	0.66 ±0.03
Exp #5	BZH7	3.0	150	1.0	150	60	1.1 ±0.04
Exp #5	BZH7	3.0	150	1.5	150	60	1.3 ±0.05
Exp #5	BZH7	3.0	150	2.5	150	60	1.5 ±0.06
Exp #5	BZH7	3.0	150	6.5	150	60	1.47 ±0.06

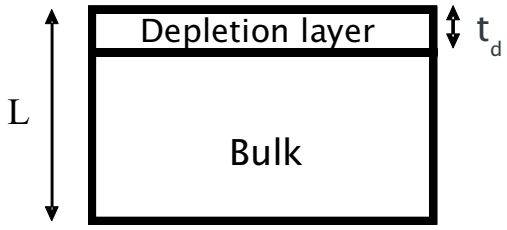

$$i = \frac{V}{R^{eq}} = \frac{V}{R_d^{eq} + R_b^{eq}}$$

$$E_{dc} = \frac{V_d}{t_d} = \frac{V}{t_d} \frac{1}{1 + \frac{R_b^{eq}}{R_d^{eq}}}$$

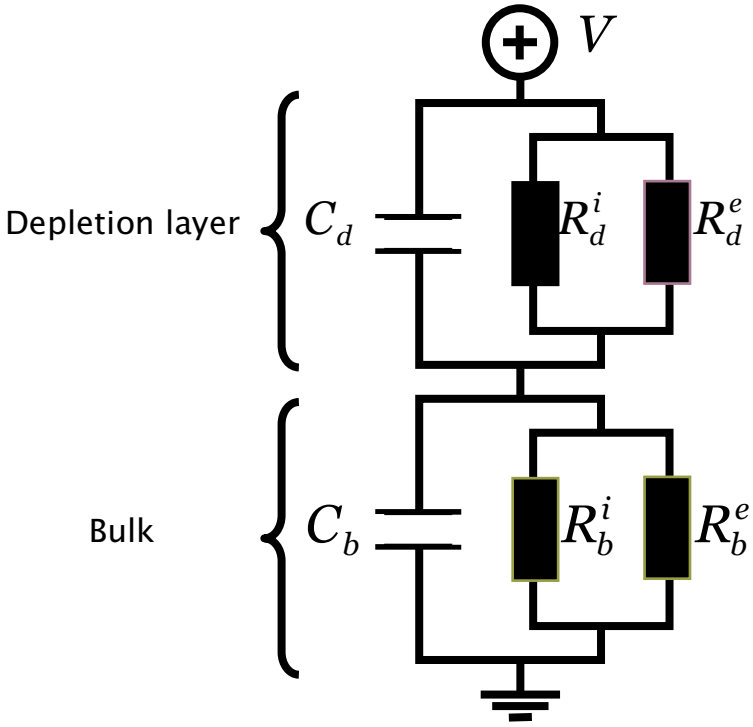

Figure 1

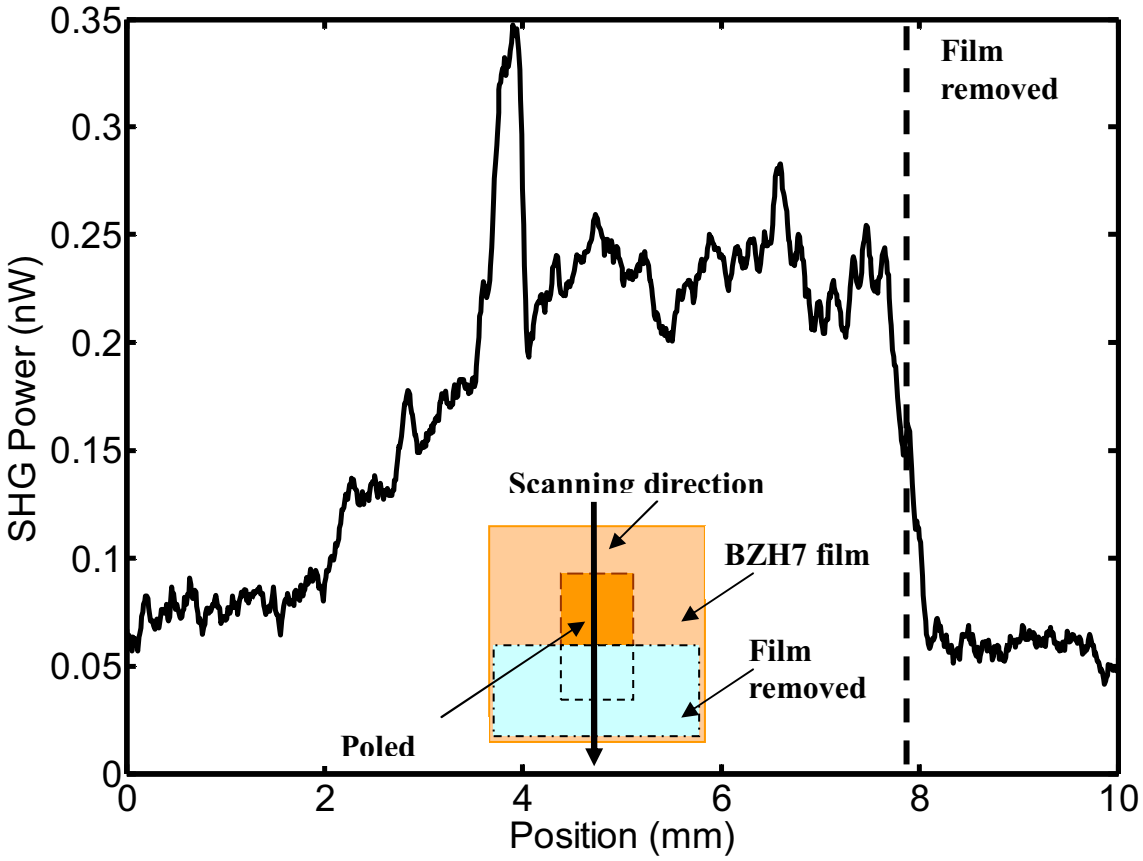
SHG Power (nW)
Position (mm)
Film
removed
Scanning direction
BZH7 film
Film
removed
Poled
0.35
0.3
0.25
0.2
0.15
0.1
0.05
0
0
2
4
6
8
10

Figure2

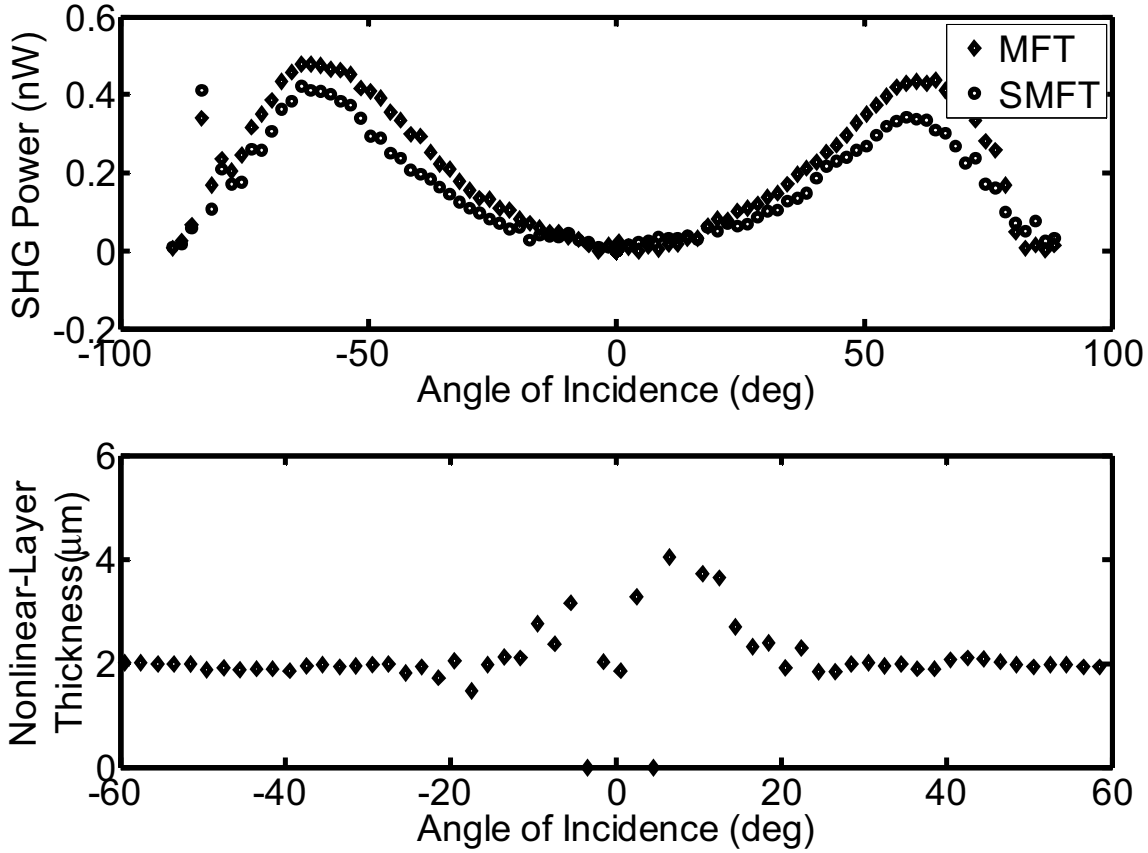
SHG Power (nW)
0.6
0.4
0.2
0
-0.2
-100
-50
0
50
100
Angle of Incidence (deg)
MFT
SMFT
Nonlinear-Layer Thickness(μm)
6
4
2
0
-60
-40
-20
0
20
40
60
Angle of Incidence (deg)

Figure 3

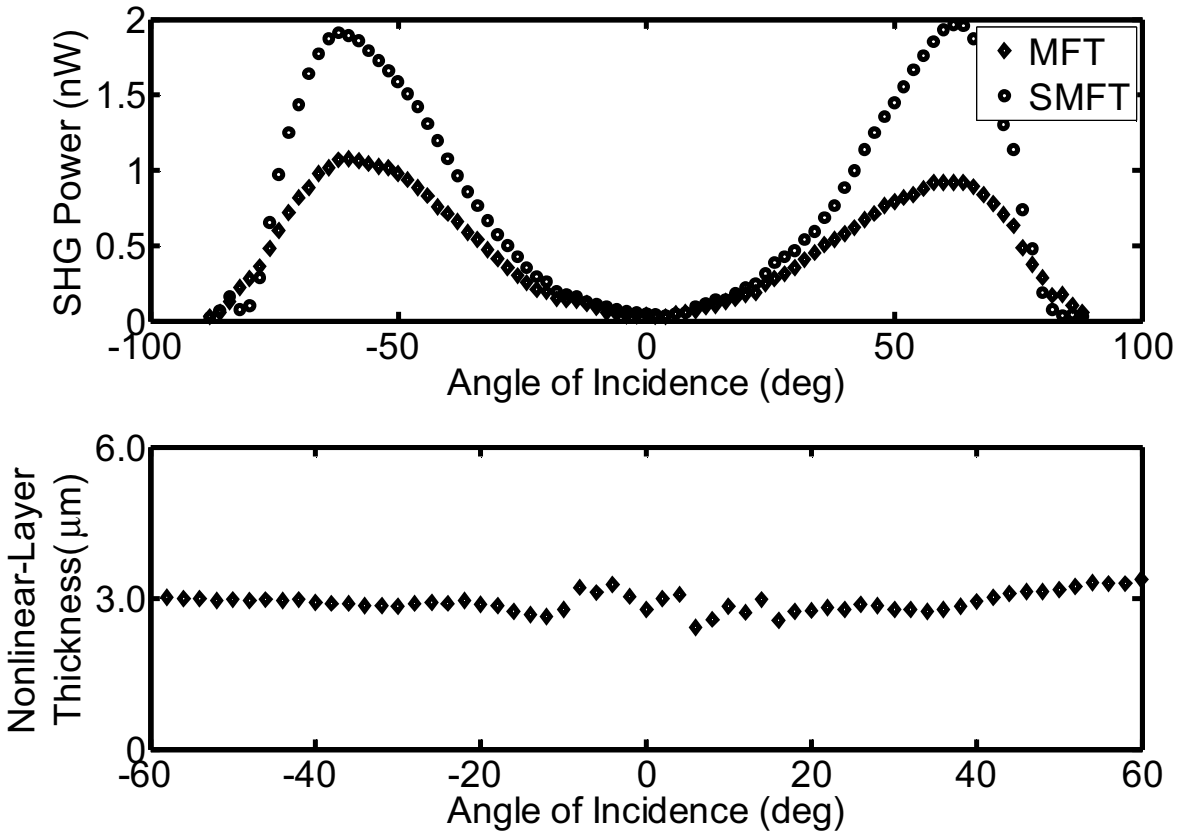
SHG Power (nW)
2
1.5
1
0.5
0
-100
-50
0
50
100
Angle of Incidence (deg)
MFT
SMFT
Nonlinear-Layer Thickness(μm)
6.0
3.0
0
-60
-40
-20
0
20
40
60
Angle of Incidence (deg)

Figure 4

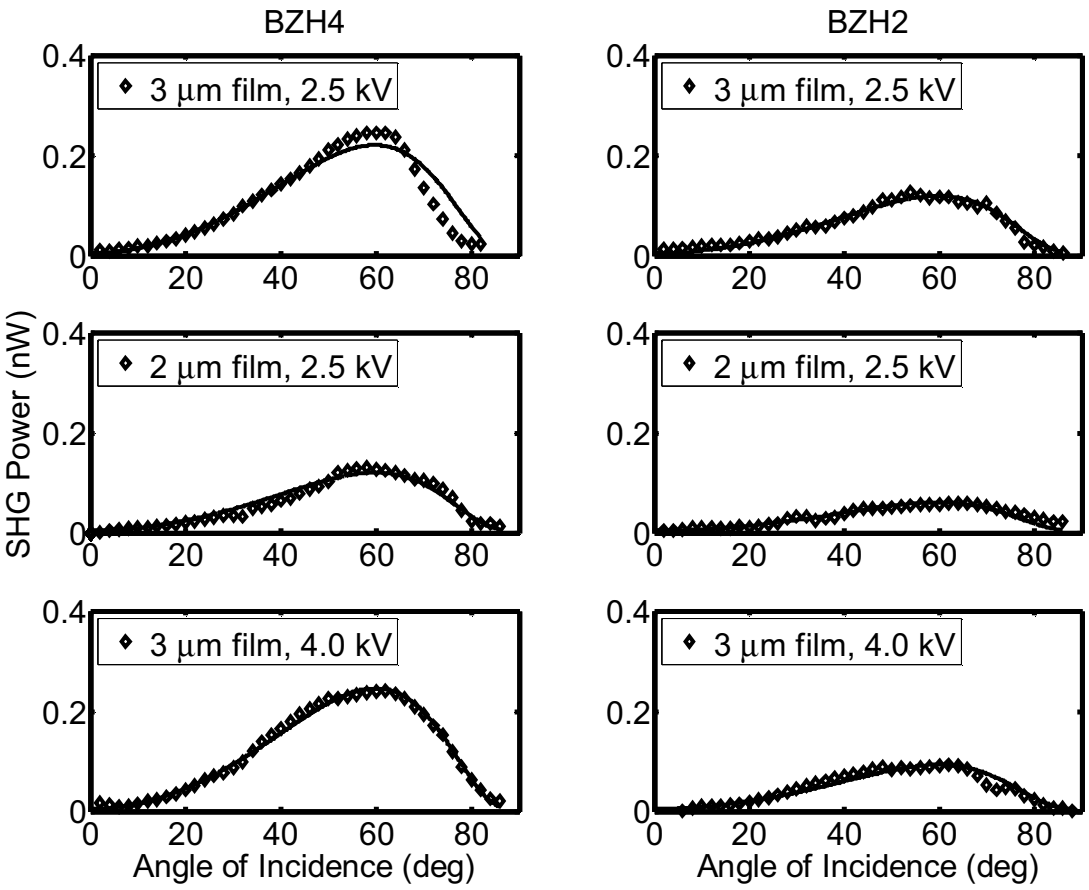
BZH4
BZH2
3 μm film, 2.5 kV
2 μm film, 2.5 kV
3 μm film, 4.0 kV
SHG Power (nW)
Angle of Incidence (deg)
0
0.2
0.4
20
40
60
80

Figure 5

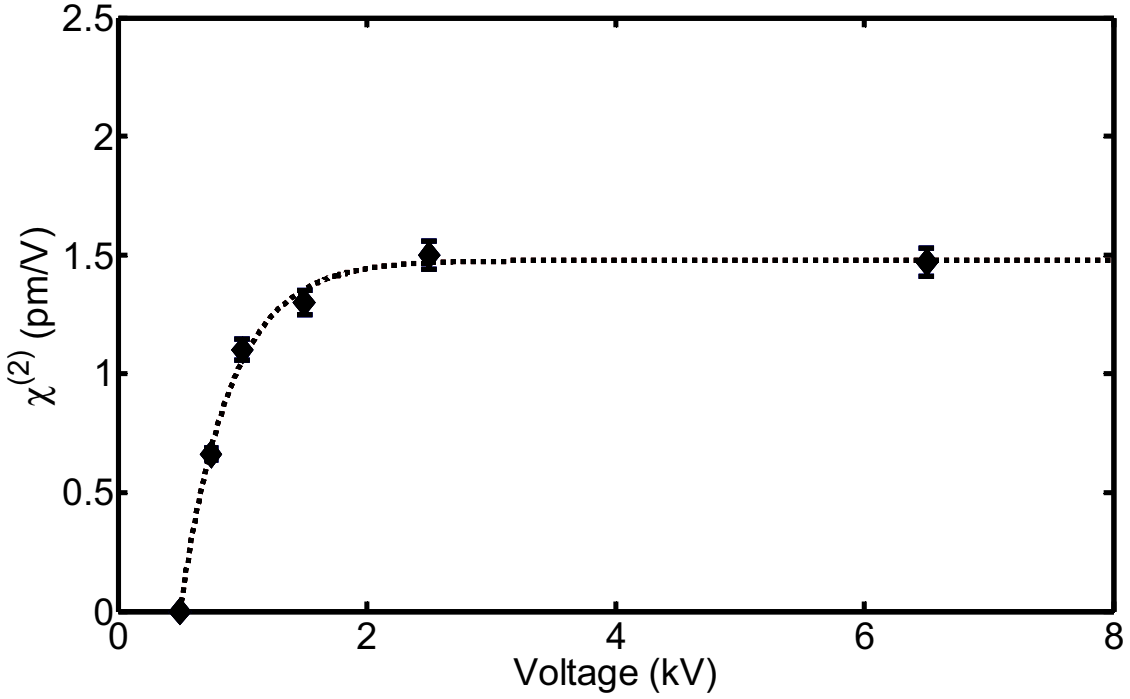

Figure 6

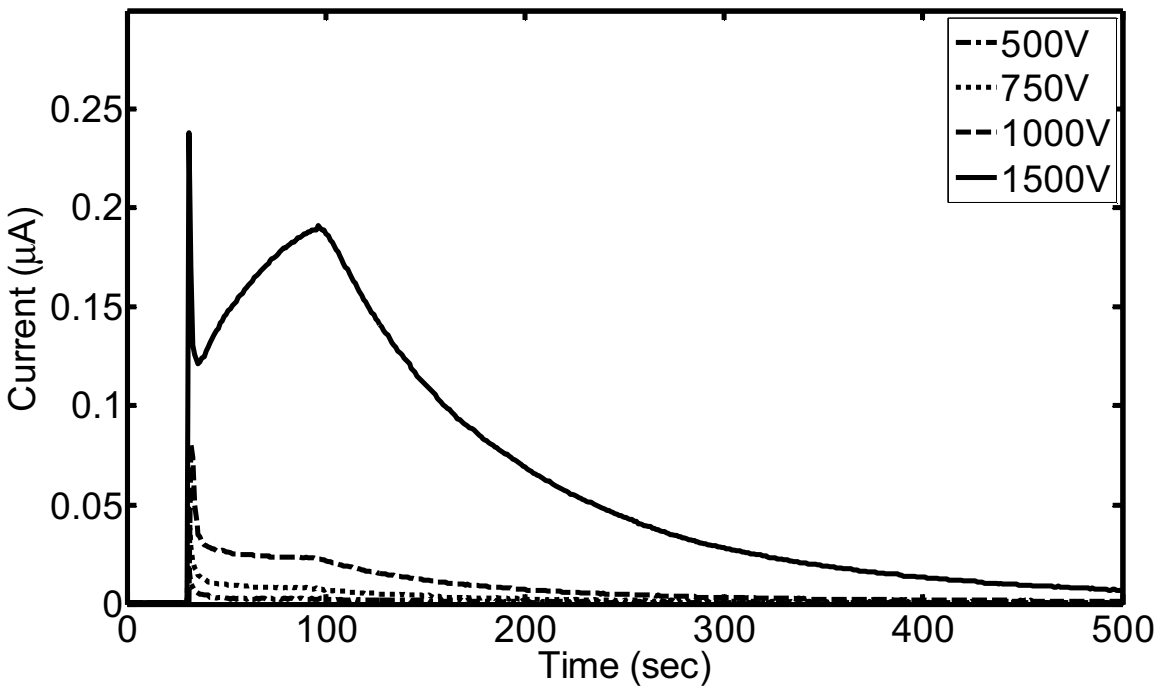
500V
750V
1000V
1500V
Current (μA)
0.25
0.2
0.15
0.1
0.05
0
0
100
200
300
400
500
Time (sec)

Figure 7

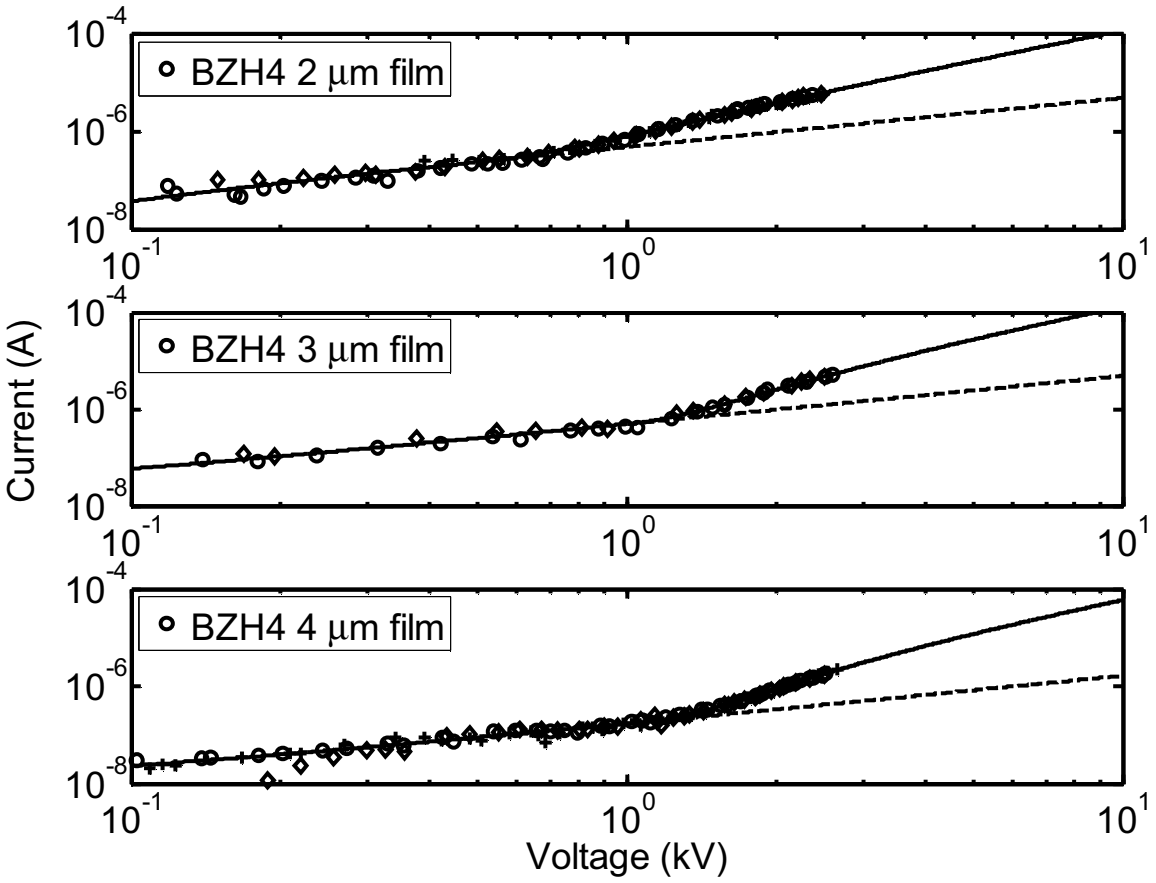
BZH4 2 μm film
BZH4 3 μm film
BZH4 4 μm film
Current (A)
Voltage (kV)
10^-4
10^-6
10^-8
10^-1
10^0
10^1

Figure 8